

A dual-head TOF-PET system for in-vivo quality control in proton therapy

P. Arce, P. Rato Mendes, N. Chamorro, J. I. Lagares, O. Vela, J. Marín
CIEMAT, Technology Department - Avda Complutense 40, Madrid, Spain

B. Aguilar, L. Irazola, J. D. Azcona
Service of Radiation Physics and Radiation Protection, Clínica Universidad de Navarra, Madrid, Spain

The SIMPROTER project

SIMPROTER: Monte Carlo simulations, experimental and clinical data to improve the quality of proton therapy treatments

- **Subproject 1:** *Monte Carlo simulations for accurate dose calculations and clinical studies of biological damage in proton therapy* (PI: Pedro Arce Dubois, CIEMAT)
 - Absolute dose calibration and fine tuning of simulation parameters for proton synchrotron at CUN
 - Microdosimetric (using Geant4-DNA) and RBE modelling in GAMOS
 - Introduce IAEA medical cross sections in GAMOS/Geant4
 - Adjust RBE data with clonogenic cell assays, compare patient data to RBE simulations
 - Collaboration with INFN-LNS (Catania, Italy) and IRSN-LDRI (Paris, France)

- **Subproject 2:** *Monte Carlo simulations and artificial intelligence for treatment verification and dose estimation in proton therapy by PET* (PI: Pedro Rato Mendes, CIEMAT)
 - Detailed simulations of real patient treatments, from beam interactions up to reconstructed PET images
 - Development of dose estimation and treatment verification methods based on PET images using AI
 - **Development and implementation of a small TOF-PET prototype system**

Duration: 4 years (09/2022 – 09/2026)

Total funding: 163.500 €

PET for treatment verification in PT (I)

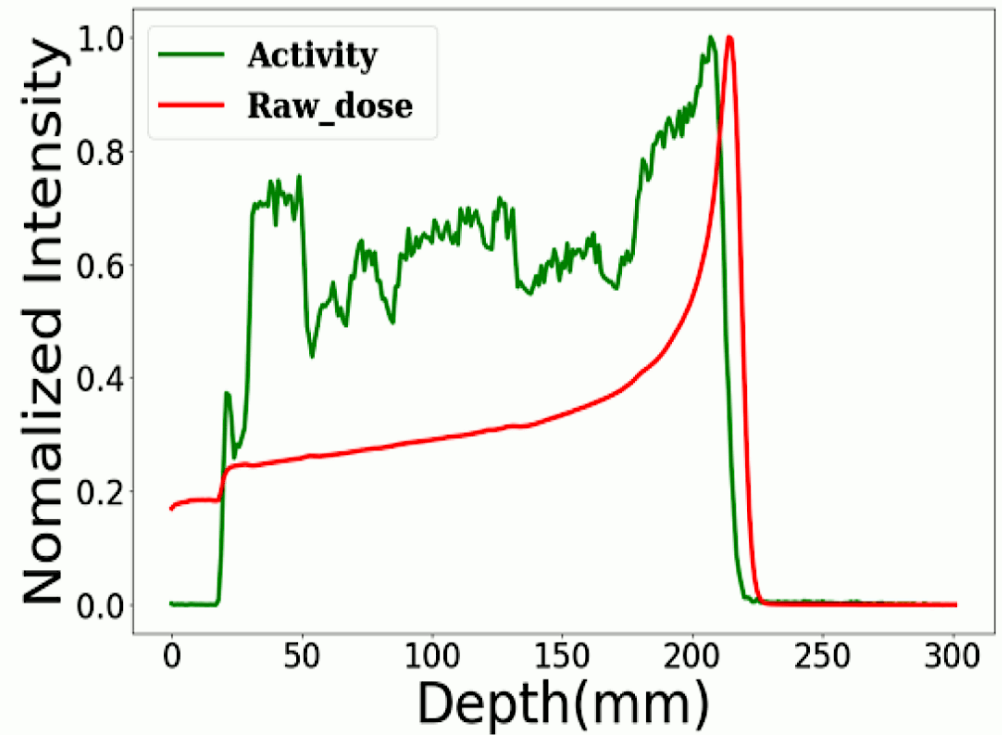
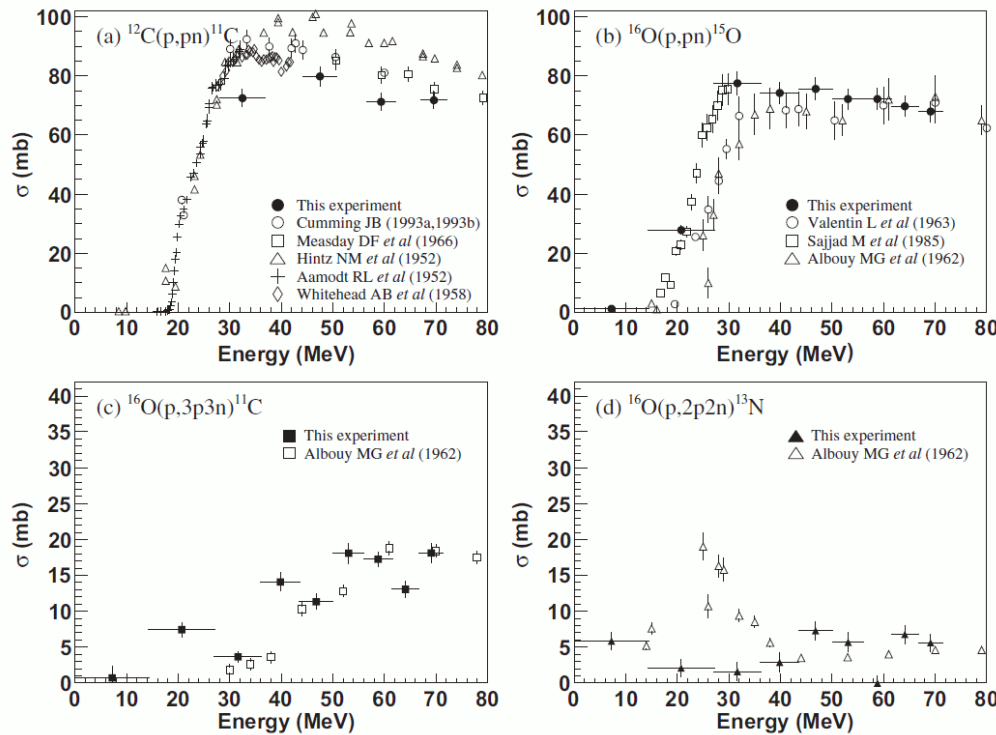
- Interactions of protons from therapeutic beam in patient's tissues induce nuclear reactions that produce positron-emitting nuclei
- The distribution of positron-emitters can thus be used to evaluate beam delivery *in vivo*

Radionuclide	Half life (min)	Reaction channels	Threshold (MeV)
^{11}C	20.39	$^{12}\text{C}(p,pn)^{11}\text{C}$ $^{14}\text{N}(p,2p2n)^{11}\text{C}$ $^{16}\text{O}(p,3p3n)^{11}\text{C}$	20.61 3.22 59.64
^{13}N	9.97	$^{14}\text{N}(p,pn)^{13}\text{N}$ $^{16}\text{O}(p,2p2n)^{13}\text{N}$	11.44 5.66
^{15}O	2.04	$^{16}\text{O}(p,pn)^{15}\text{O}$	16.79

- The most intense positron emitters ^{11}C , ^{13}N and ^{15}O have short half lives, PET imaging should start as soon as possible, during irradiation (if feasible) or immediately after
- Biological washout of positron emitters is also minimized by early image acquisition
- The use of dedicated PET detectors close to the patient improve detection efficiency compared to in-room or remote whole body PET scanners later (10 to 30 min) imaging

PET for treatment verification in PT (II)

- The cross-sections for generating positron-emitters fade out at lower proton energies, and are negligible at the Bragg peak, where local dose deposition is at its maximum
- As a consequence, the distribution of positron emitters and the dose distribution are not directly correlated, and the distal fall-offs (ranges) usually differ by a few mm



Taken from T. Akagi et al., Radiat Meas 59 (2013) 262-269

Taken from C. Liu et al., Phys Med Biol 64 (2019) 175009

PET for treatment verification in PT (III)

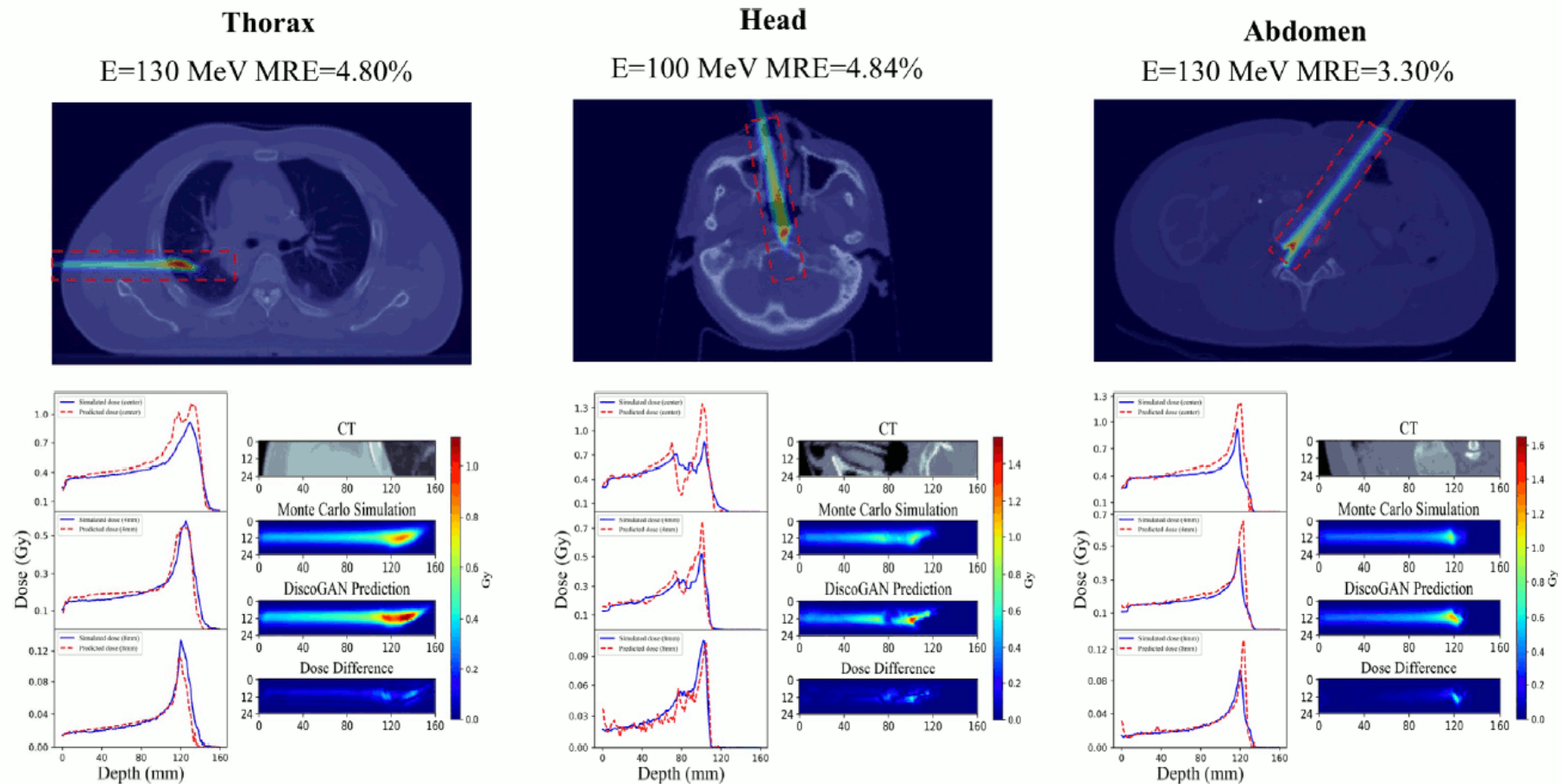
Possible approaches to the use of PET for treatment verification in PT:

- **Estimate delivered dose and compare with prescribed dose**
 - Needs accurate modelling of beam and treatment delivery parameters, as well as materials and densities from patient CT, interaction cross-sections and correct calibration of PET detectors
 - May be performed by Monte Carlo calculations and/or artificial intelligence methods
- **Comparison between different sessions of the same treatment**
 - PET images from different treatment sessions should be similar
 - Comparing PET images acquired under the same circumstances is less dependent on accurate beam, patient and detector modelling
 - Differences in PET images could be due to mispositioning, movement or changes in patient anatomy throughout the course of treatment, that may require corrective measures

Both approaches will be studied within SIMPROTER project

Treatment verification by estimating dose from PET (I)

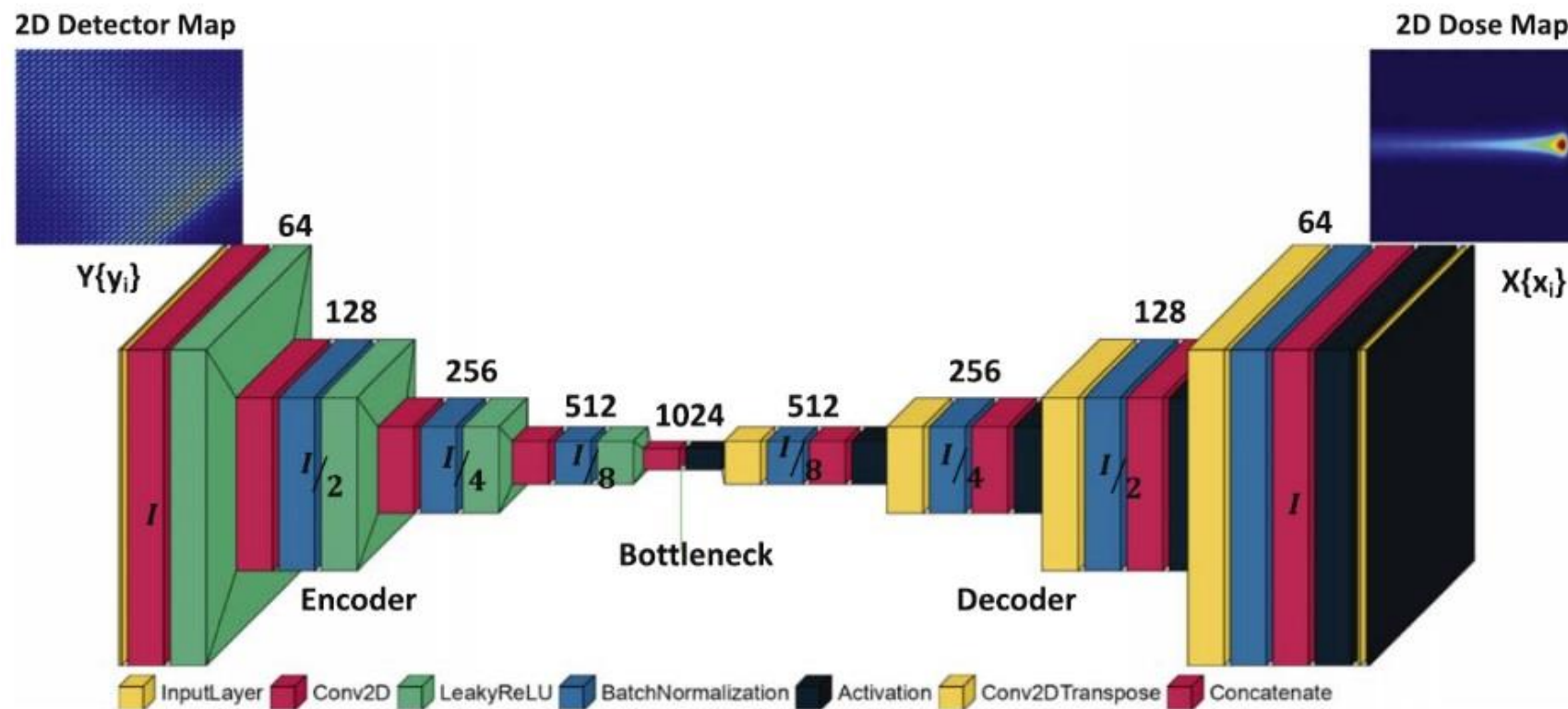
- Example of AI use (Generative Adversarial Network, GAN) for dose estimation from Monte Carlo simulations using patient CT and PET images of induced positron-emitter activity



Taken from X. Zhang et al., Med Phys 48 (2021) 2646-2660

Treatment verification by estimating dose from PET (II)

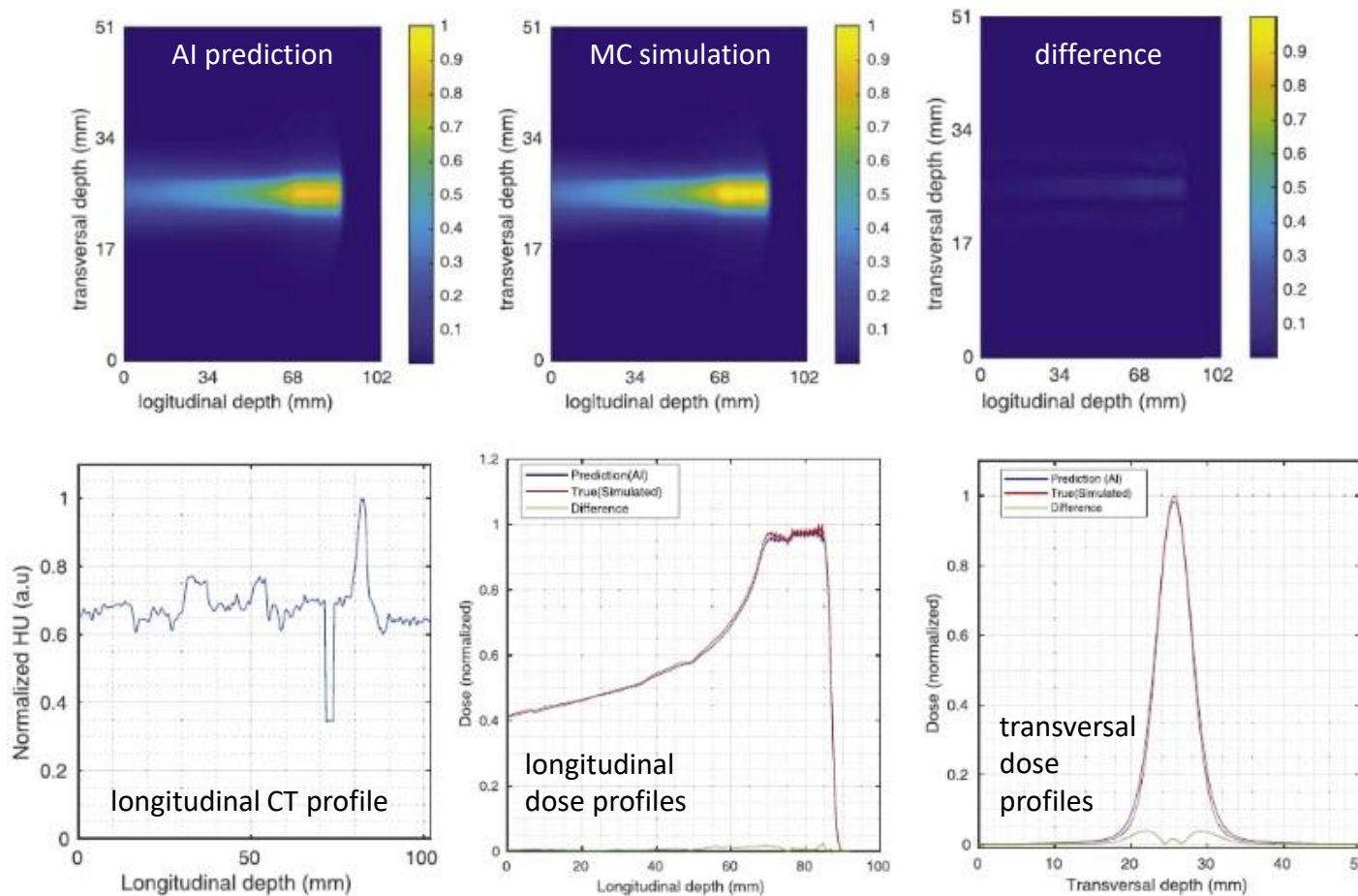
- Example of AI use (conditional GAN) for dose estimation from Monte Carlo simulations
- Direct mapping from detector coincidence maps to dose (2D only)



Taken from A. U. Rahman et al., Phys Med Biol 67 (2022) 185010

Treatment verification by estimating dose from PET (II)

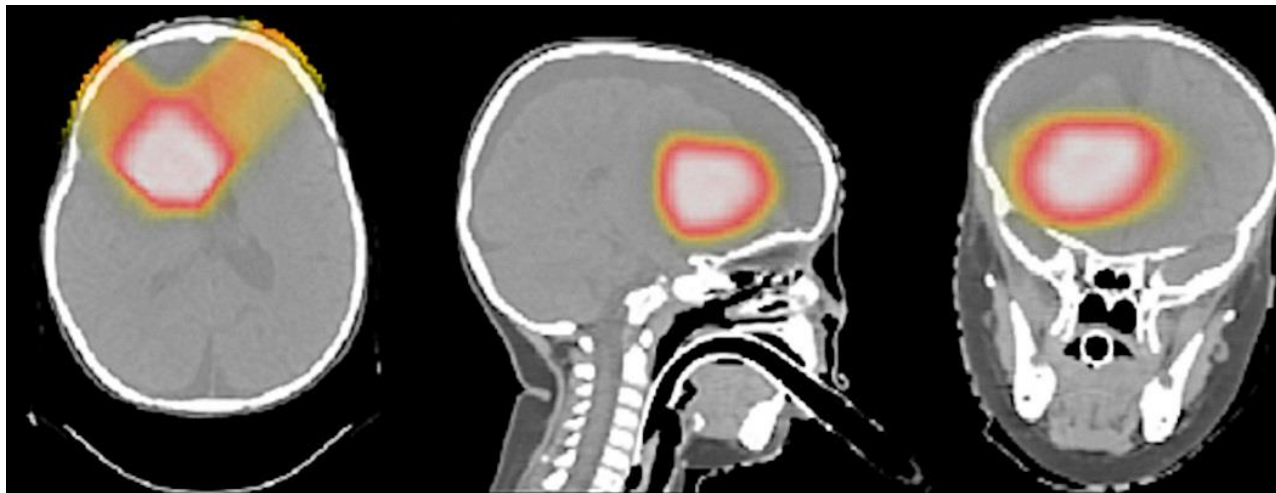
- Example of AI use (conditional GAN) for dose estimation from Monte Carlo simulations
- Direct mapping from 2D coincidence maps to dose (2D only)



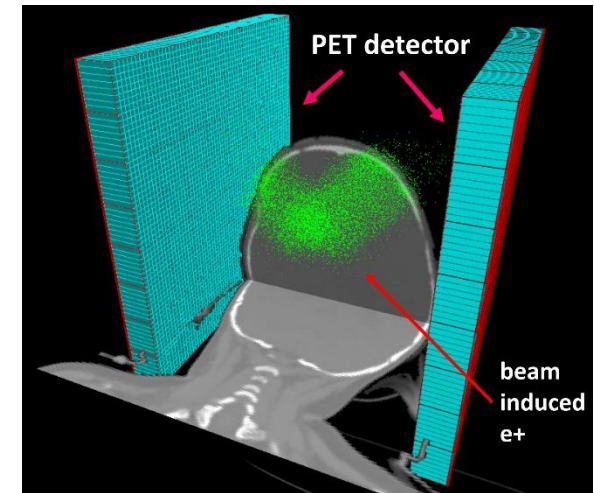
Adapted from A. U. Rahman et al., Phys Med Biol 67 (2022) 185010

Treatment verification by comparison of PET images (I)

- **Monte Carlo simulations** by our group using GAMOS 6.3.0 and real patient treatment plans
- Dedicated dual head PET detector with $\sim 20 \times 20 \text{ cm}^2$ active area
 - 8 x 8 detector modules per head
 - Each module composed of a Hamamatsu S13361-3050AE-08 SiPM array and a LYSO:Ce array with $3.14 \times 3.14 \times 20 \text{ mm}^3$ elements and 1:1 coupling (optical photons not simulated)
 - HRFlexToT front-end readout enabling time-of-flight PET (200 ps CTR)



Prescribed dose from treatment planning system:
axial, sagittal and coronal views (left to right)



Detectors placed close to patient
showing induced positron activity

Treatment verification by comparison of PET images (II)

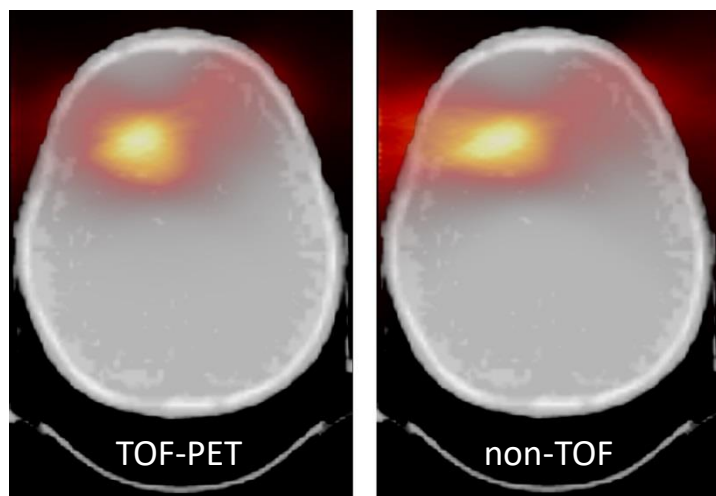
Monte Carlo simulation of two real patient treatments

- Head and neck patient with two orthogonal proton fields (shown on previous slide)
- Craniospinal irradiation with one proton field (only lower spine)
- Changes in PET images were artificially introduced by modulating beam energies in order to evaluate the detectors' performance in detecting such changes
 - Originally prescribed treatment used as reference
 - Different treatments were simulated with 1, 2, 5 and 10 mm range shifts on the patient
 - Several instances of each treatment simulated with different random seeds to perform a statistical analysis
- PET images were compared by determining the distal fall-off of positron activity profiles along lines parallel to the primary beams, and also by calculating the Pearson correlation coefficient on volumes of interest

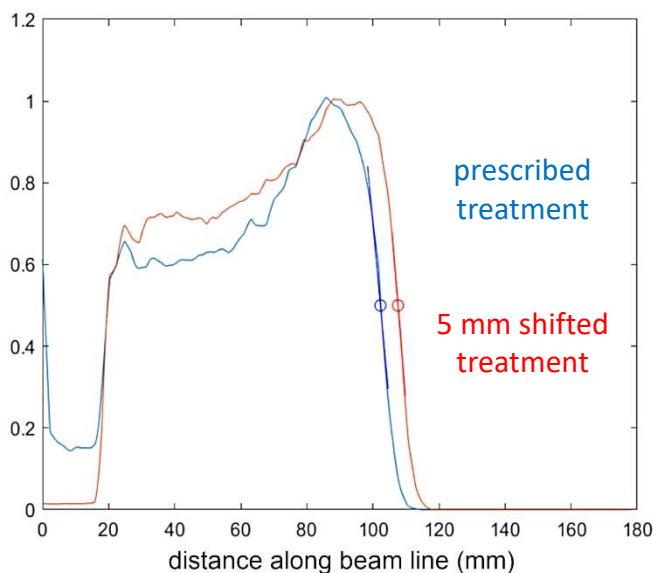
Treatment verification by comparison of PET images (III)

Head and neck treatment – main results

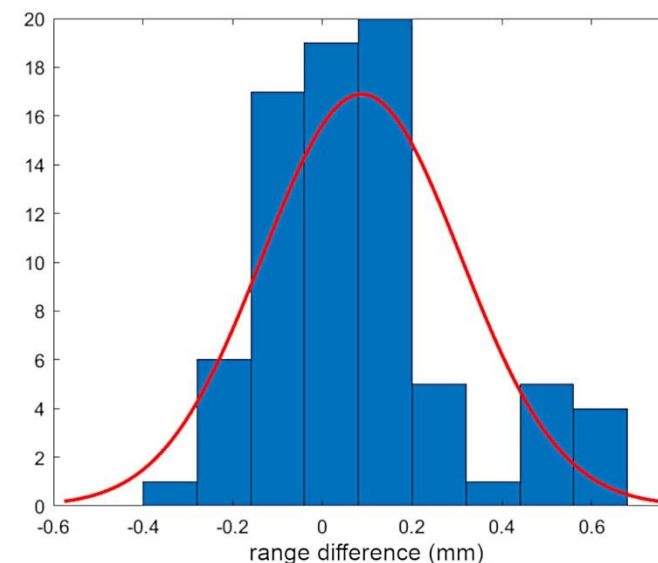
- Good image consistency from different random seeds for a given treatment
- TOF-PET reconstruction improves image quality (as expected for face-to-face detectors)
- Over 80% sensitivity and specificity for 1 mm range shifts, 100% for larger ones



axial views of reconstructed activity (detectors at the sides of patient's head)



activity profiles for an original treatment and a 5 mm-shifted treatment



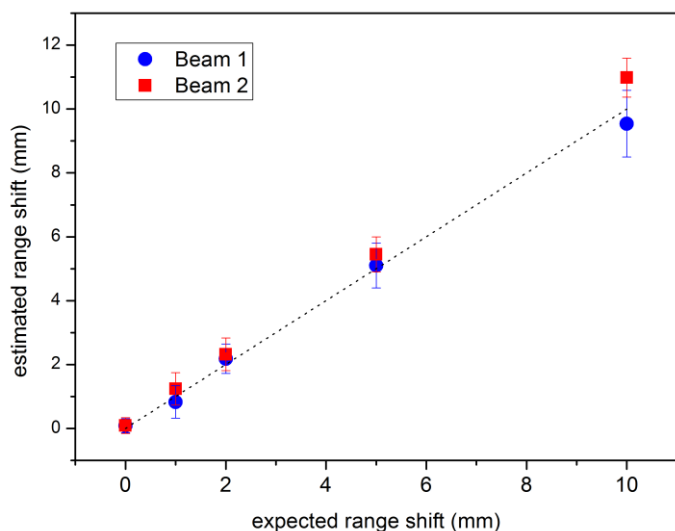
average range shift differences for comparisons between all instances of the prescribed treatment

P. Arce et al., presented at IEEE NSS MIC RTSD 2022

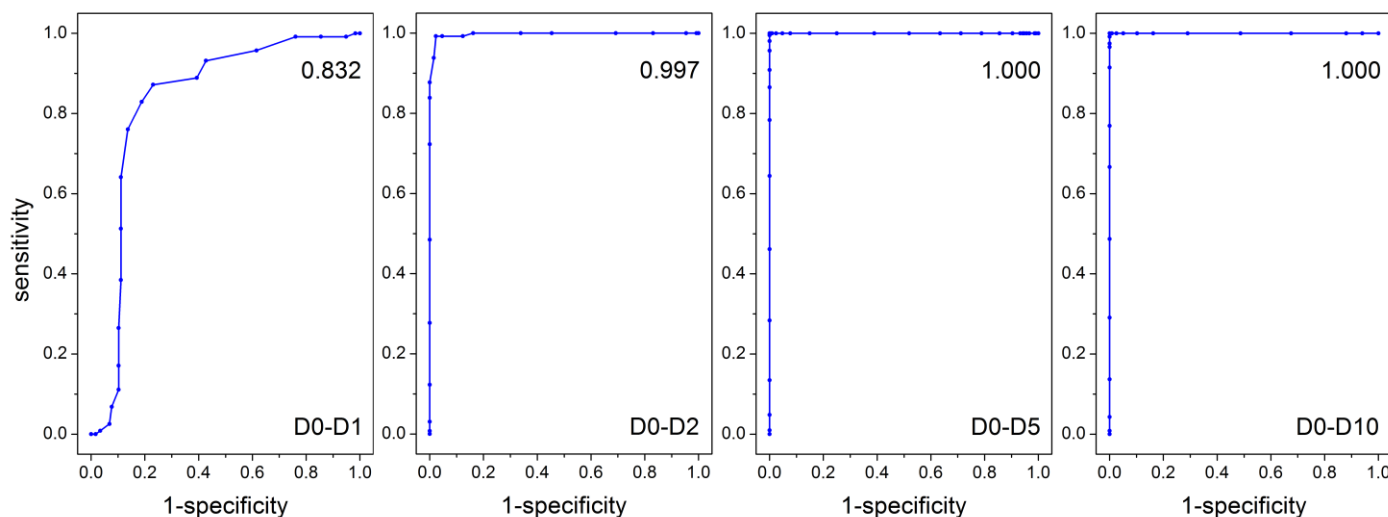
Treatment verification by comparison of PET images (III)

Head and neck treatment – main results

- Good image consistency from different random seeds for a given treatment
- TOF-PET reconstruction improves image quality (as expected for face-to-face detectors)
- Over 80% sensitivity and specificity for 1 mm range shifts, 100% for larger ones



average estimated vs expected range shifts for all treatment comparisons

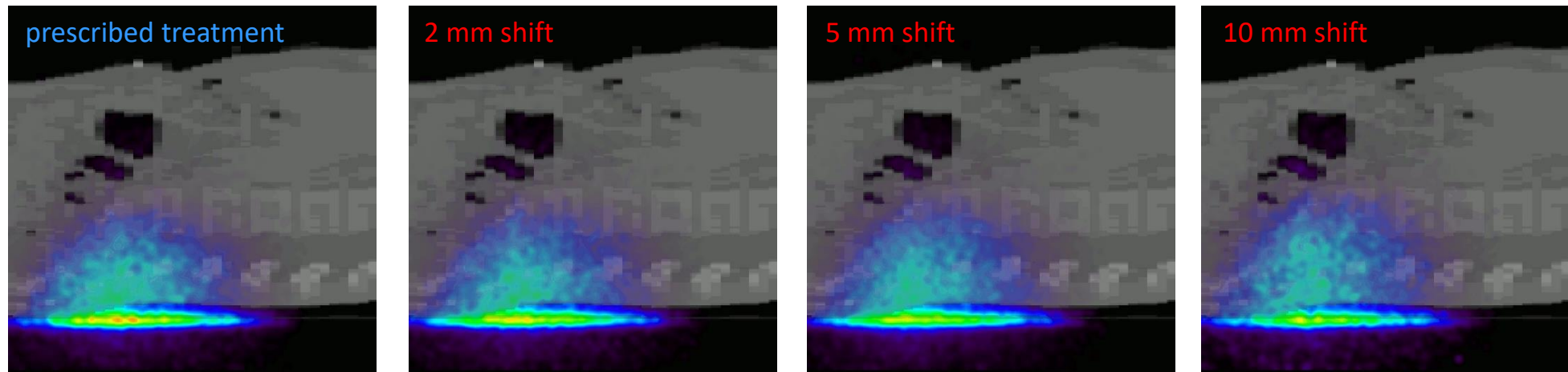


ROC curves for 1, 2, 5 mm and 10 mm expected range shifts (left to right)
Area under the curve (AOC) values also included

Treatment verification by comparison of PET images (IV)

Craniospinal irradiation – main results

- Noisier images from less induced activity and increased separation of PET detectors
- Comparison based on Pearson correlation less performing than range estimation
- TOF-PET reconstruction less important in this case due to detector positioning



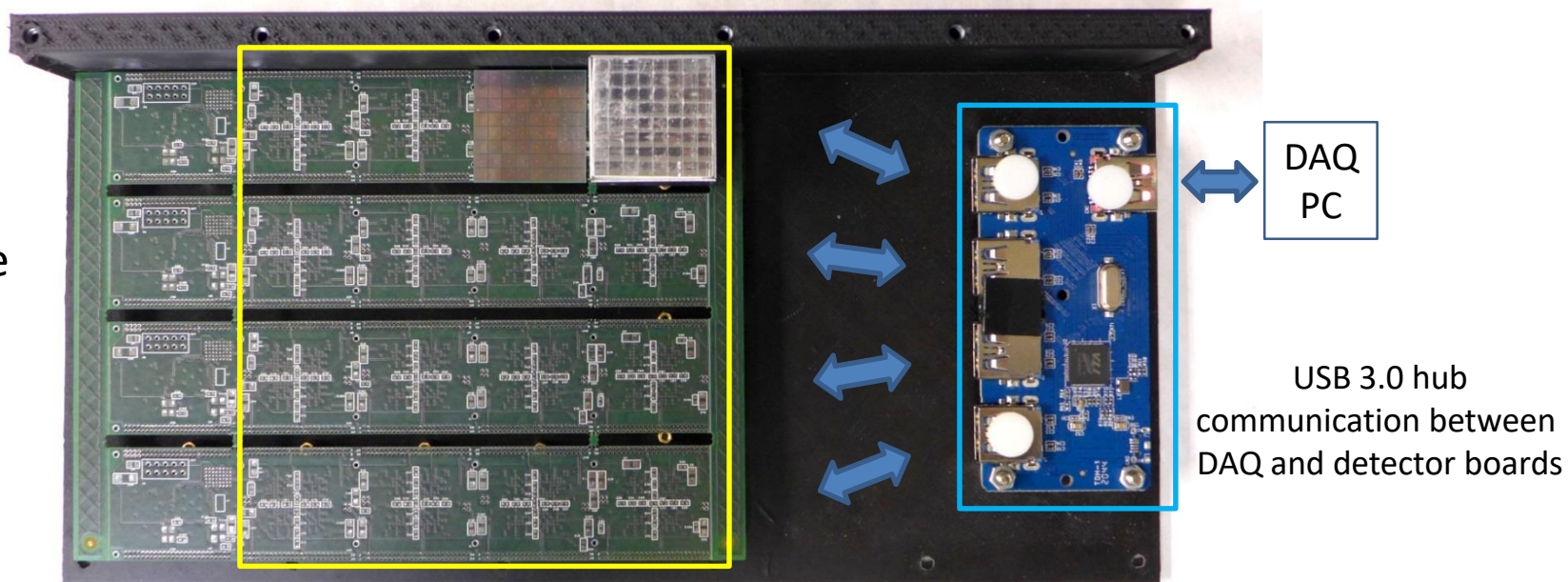
Reconstructed sagittal PET images overlaid on the craniospinal patient CT for original treatment and 2, 5 and 10 mm shifts. Beam was administered through the lumbar region of the patient (from bottom to top), inducing activity on the patient bed.

P. Arce et al., presented at IEEE NSS MIC RTSD 2022

SIMPROTER prototype PET detector

- Dedicated dual head PET detector with $\sim 10 \times 10 \text{ cm}^2$ active area
 - 4 x 4 detector modules per head (smaller than simulated detector due to budget limitations)
 - Each module composed of a Hamamatsu S13361-3050AE-08 SiPM array and a LFS/LYSO:Ce array with $3.14 \times 3.14 \times 20 \text{ mm}^3$ elements and 1:1 coupling
 - HRFlexToT front-end readout enabling time-of-flight (TOF-)PET
 - 3x piggy-back interconnected PCBs for SiPM mounting, USB 3.0 communications and FPGAs

first prototype detector box (in progress)



$\sim 10 \times 10 \text{ cm}^2$ active detector area
 4 x 4 detector modules
 LFS/LYSO:Ce arrays + SiPM arrays

DAQ PC
 USB 3.0 hub communication between DAQ and detector boards

Summary and outlook

- SIMPROTER project recently approved with two overlapping lines of research
 - *Monte Carlo simulations for accurate dose calculations and clinical studies of biological damage in proton therapy*
 - *Monte Carlo simulations and artificial intelligence for treatment verification and dose estimation in proton therapy by PET*
- Monte Carlo simulation results highlight the potential of using a dedicated small PET detector for treatment verification in protontherapy
- We will develop a small PET prototype detector and dose estimation methods based on AI in collaboration with a clinical protontherapy centre aiming at *in vivo* treatment verification based on PET imaging



UNIÓN EUROPEA



FONDO EUROPEO DE
DESARROLLO REGIONAL

“Una manera de hacer Europa”



Thank you for your attention!

pedro.rato@ciemat.es

Grants PID2021-127902OC-C21 and PID2021-127902OC-C22 funded by MCIN/AEI/10.13039/501100011033 and “ERDF A way of making Europe”